Computers in Biology and Medicine 142 (2022) 105232

Contents lists available at ScienceDirect

Computers in Biology and Medicine

journal homepage: www.elsevier.com/locate/compbiomed

Main glucose hepatic fluxes in healthy subjects predicted from a phenomenological-based model

Carlos E. Builes-Montaño [a], Laura Lema-Perez [b,*], Jose Garcia-Tirado [c], Hernan Alvarez [d]

[a] Hospital Pablo Tobón Uribe, Facultad de Medicina, Universidad de Antioquia, Medellín, Colombia
[b] Department of Engineering Cybernetics, Norwegian University of Science and Technology (NTNU), Trondheim, Norway
[c] Center for Diabetes Technology, University of Virginia, Charlottesville, VA, USA
[d] Escuela de Procesos y Energía, Kalman Research Group, Facultad de Minas, Universidad Nacional de Colombia, Medellín, Colombia

ARTICLE INFO

Keywords:
Mathematical model
Diabetes mellitus
Glucose metabolism
Liver

ABSTRACT

Background: The liver has a unique role in blood glucose regulation in postprandial, postabsorptive, and fasting states. In the context of diabetes technology, current maximal models of glucose homeostasis lack a proper dynamical description of main glucose-related fluxes acting over and from the liver, providing a rather simplistic estimation of key quantities as endogenous glucose production and insulin and glucagon clearance.
Methods: Using a three-phase well-established phenomenological-based semi-physical modeling (PBSM) methodology, we built a detailed physiological model of hepatic glucose metabolism, including glucose utilization, endogenous glucose production through gluconeogenesis and glycogenolysis, and insulin and glucagon clearance. Mean absolute errors (MAE) were used to assess the goodness of fit of the proposed model against the data from three different in-vivo experiments -two oral glucose tolerance tests (OGTT) and a mixed meal challenge following overnight fasting-in healthy subjects.
Results: Needing little parameter calibration, the proposed model predicts experimental systemic glucose mean ± std 5.4 ± 5.2, 7.5 ± 6.8, and 7.5 ± 7.5 mg/dL, in all three experiments. Low MAEs were also obtained for insulin and glucagon at the hepatic vein.
Conclusions: The quantitative concordance of our model to the experimental data exhibits a potential for its use in the physiological study of glucose liver metabolism. The model structure and parameter interpretability allow the union with other semi-physical models for a better understanding of whole-body glucose homeostasis and its use in developing diabetes technology tools.

1. Introduction

In healthy subjects, blood glucose levels are maintained within a narrow range of around 70–110 md/dL thanks to a sophisticated natural closed feedback loop involving mainly the gastrointestinal (GI) tract, pancreas, kidneys, liver, and peripheral tissues, despite complex disturbances caused mainly by glucose-containing meals and a lack of physical activity. In this complex orchestration, the liver plays a key role, acting as a buffer in all fasting, postprandial, and post-absorptive states through hepatic glucose production and utilization (glycogenolysis, glycolysis, glycogenesis, and gluconeogenesis) [1,2]. In this complex and intertwined metabolic process, insulin and glucagon (viz. the glucose-lowering hormone and its antagonist) are used and degraded.

Insulin and glucagon are the main regulatory hormones in glucose homeostasis. In what seems an indirect process, insulin acts on adipose tissue lipolysis by suppressing free fatty acids, which in turn modulate (suppress) hepatic glucose production [1]. Glucagon, on the other hand, promotes hepatic glycolysis as a response to hypoglycemia. Moreover, major insulin and glucagon clearance takes place in the liver [3,4], being the latter process less known and quantified in humans than the former [3].

Understanding hepatic glucose metabolism is key in explaining the main mechanisms of glucose regulation and to provide useful and actionable insight to treat impaired glucose conditions such as Type 1 Diabetes (T1D) and Type 2 Diabetes (T2D). Although T1D (a.k.a. insulin-dependent diabetes) is a widespread autoimmune disease, the

* Corresponding author.
E-mail addresses: esteban.builes@udea.edu.co (C.E. Builes-Montaño), laura.l.perez@ntnu.no (L. Lema-Perez), jg2bt@virginia.edu (J. Garcia-Tirado), hdalvare@unal.edu.co (H. Alvarez).

https://doi.org/10.1016/j.compbiomed.2022.105232
Received 21 September 2021; Received in revised form 8 January 2022; Accepted 9 January 2022
Available online 14 January 2022

prevalence of T2D is increasing at alarming rates due mainly to the modern lifestyle, among other well studied causes [5]. According to the International Diabetes Federation (IDF) as of 2019, 463 million people had diabetes with a 51% estimated increase in 2045 (~ 700 million) [5].

Digital therapeutics have emerged in recent years as a promising alternative for diabetes care [6,7] This encompasses a variety of tools including apps for decision support systems and automatic insulin delivery (a.k.a. the artificial pancreas) and the widespread use of the Internet to provide specific targeted treatment. Behind-the-scenes, mathematical models of (or related to) glucose homeostasis play a key role in the design, testing, and implementation of these technologies. Specifically, computer simulation has, undoubtedly, accelerated the development of such technologies and has, for the specific case of the artificial pancreas, replaced the animal trials in the preclinical testing phase [8,9].

The mathematical representation of glucose homeostasis either in healthy subjects or in T1D/T2D has been a subject of intense research for over 40 years now [10,8]. Although numerous investigations have contributed to building the body of knowledge regarding such a complex mechanism, there is still some important that remains unknown/not thoroughly understood; e.g., the effect of different types of physical activities in endogenous glucose production and glucose utilization, glucagon metabolism, and accurate dynamical representations of insulin and glucagon secretion, among others.

Despite the key role of the liver in glucose homeostasis, there is, as yet, no accurate simulation model of the glucose-related hepatic metabolism, representing known physiological aspects and with the possibility of being individualized (identified) with specific field data. In this work, we propose a novel physiologic mathematical model of the glucose hepatic metabolism developed by a well established modeling methodology [11,12]. Key aspects such as Endogenous Glucose Production (EGP), hepatic glucose utilization, and insulin and glucagon clearance are integrated into this mathematical model together with metabolic and hormonal regulation. We show the prediction ability of the model by replicating in the simulation the results from three different experimental setups available in the literature [13,14,15] for a median hypothetical subject with minimal parameter calibration.

2. Role of the liver in glucose metabolism

The liver receives the mainstream of nutrients, including carbohydrates, right after reaching the bloodstream from the intestine. As such, it dampens both carbohydrate and several hormone fluxes through different pathways [16]. Specifically, glucose enters hepatocytes via Glucose transporter 2 (GLUT2), a bidirectional transporter that allows passive entry and exit by concentration difference rather than by insulin action, a common mechanism elsewhere [17].

Once inside the hepatocytes, glucose can be stored as glycogen, used to produce energy or fatty acid synthesis [18]. The first step in hepatic glucose metabolism is its phosphorylation to Glucose 6 phosphate (G6P) by Glucokinase (GK), a low molecular weight enzyme that is not inhibited by its product, G6P, and has a lower affinity for glucose compared to other hexokinases [19]. G6P can then undergo isomerization to Glucose 1 phosphate (G1P) or Fructose 6 phosphate (F6P) or oxidation to gluconolactone. In the postprandial period, about 50% of the ingested glucose will be converted to glycogen through the G1P pathway (direct route) [20], but the storage capacity of glycogen in the liver is limited and excess glucose from the diet goes in part to fatty acid synthesis [21]. Also, in the postprandial period, the liver is not predominantly oxidative, which causes the amount of glucose to be metabolized through the F6P pathway to be very small [22].

GK is a widely regulated enzyme in the liver; whole activation occurs by Fructose 1 phosphate (F1P) and its gene transcription is subject to hormonal regulation (insulin and glucagon). Direct and indirect inhibition are mediated by Glucokinase regulatory protein (GKRP) and Fructose 1–6 biphosphate (FBP), respectively. In the presence of F6P, GKRP binds to form an inhibitory complex, which separates in the presence of F1P losing its activity. During the postprandial period, F1P levels are high, facilitating the flow of glucose into the cell by concentration difference [23]. Also, GK concentration is higher in the cytoplasm, where high levels of insulin increase its transcription [24]. In contrast, in the post absorptive period, GK remains inside the nucleus from which it cannot exert its action on glucose [25], where high levels of glucagon repress its transcription.

After an oral carbohydrate intake, the activity of Glucose 6 phosphatase (G6Pase) is partially suppressed by insulin [26], but glucose stimulates G6Pase and, paradoxically, this seems to be necessary to maintain high levels of G6P, which in turn, is needed to switch from glycogenolysis to glycogenogenesis [27]. The mechanism used by the liver to transition from being a glucose-producing organ to a glucose storing organ is similar to that of a switch; it is a matter of debate whether the effector is glucose or insulin. However, the action is parallel to glucose concentration. In spite of this, insulin is necessary to achieve the maximum glycogen concentration in the presence of glucose [28]. Although glycogen's main route comes directly from the metabolism of ingested carbohydrates, glucose produced via gluconeogenesis may represent up to 25% of the total amount of glycogen production in fed and fasting states [20].

3. Methods

In this section, we discuss the steps taken to build a phenomenological-based semi-physical model (PBSM) accounting for the role of the liver in glucose homeostasis. We used a three-phase methodology to build the model [29]. In the pre-construction phase, we described the process to be modeled and the model's objective, proposed a modeling hypothesis, stated the level of detail, and defined the process systems. In the construction phase, we applied the conservation principle, obtaining the model's basic structure. We then classified the symbols forming the equations selected for the basic structure as variables, structural parameters, and constants. We used constitutive and assessment equations to define the unknown parameters of every process system. A constitutive equation approximates the response of a physical quantity to external stimuli using a law or principle. An assessment equation is a mathematical relation to assess a parameter's numerical value. In the final step of the construction phase, the model's degrees of freedom are verified. In the final phase, we constructed a computational model and contrasted its results against experimental data available in the literature. Examples of previous models following this methodology are available elsewhere [30,31,32,11,12]. This methodology makes it possible to build a mathematical model based on the current knowledge of physiology, with interpretable parameters and a unique and modular basic structure. This enables the model to be used for different purposes.

3.1. Model pre-construction

3.1.1. Process description and model aim

Unlike any other organ, the liver receives blood from two sources, the portal vein and the hepatic artery. The blood from the portal vein flows from the splanchnic bed. In the post-absorptive state, the species concentrations resemble the ones in the systemic circulation. After a carbohydrate-containing meal, portal vein blood contains a high concentration of glucose, fatty acids, or amino acids, depending on the type of food. Oxygen-rich blood from the peripheral circulation enters via the hepatic artery with a more or less constant glucose concentration. The hepatic artery's terminal branches and the portal vein (portal triad) empties its blood content into small channels called sinusoids. These low-pressure vascular tunnels carry blood from the portal triads toward the central hepatic vein. One hepatic lobule contains millions of sinusoids lined by highly fenestrated endothelial cells and surrounded by hepatocytes, as depicted in Fig. 1. This configuration allows the

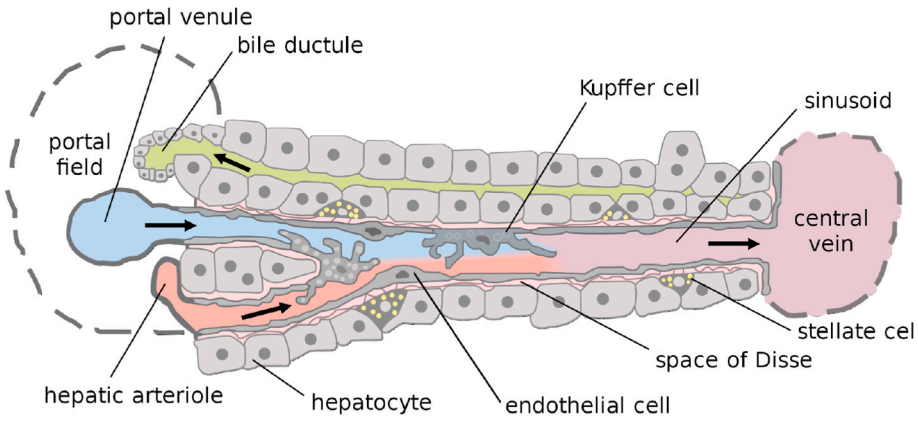

Fig. 1. Representation of a liver sinusoid. Figure reproduced from Frevert, U. et al. [33], in line with Creative Commons Attribution License - CC BY 4.0..

exchange of nutrients, metabolism-related substances, and oxygen to flow between blood and the hepatocytes.

In healthy individuals, a blood glucose concentration of around 90 mg/dL (~ 72–180 mg/dL) is maintained, in part, due to the liver's ability to store and produce glucose. As described earlier, the glucose storage process is mainly active in the postprandial period where 50% of the ingested glucose is converted to glycogen [20]. But most glucose (both ingested and circulating) is used in other metabolic routes such as fat production. In fasting, the liver breaks down glycogen to supply glucose and can produce glucose from non-hexose precursors such as lactate [34]. Part of that circulating glucose is used by the liver to supply its energy requirements.

All the physiologic phenomena of glucose metabolism in the liver, e.g., *glycolysis* (energy production), *glycogenesis* (glycogen storage), *glycogenolysis* (glycogen breakdown to produce glucose), and *gluconeogenesis* (glucose production from non-hexose precursors) coexist and are regulated by the intermediated products of different reactions such as G6P and by hormones secreted by the pancreas (insulin and glucagon). In the postprandial period, high levels of insulin and glucose promote glucose storage and decrease glucose production. During fasting, low circulating glucose concentration, decreasing/increasing insulin/glucagon production from the pancreas, blocks glucose storage and facilitates endogenous glucose production (EGP).

In our model, all four described physiological phenomena as well as the regulatory influence of insulin and glucagon on the liver are considered in both postprandial and fasting states.

3.1.2. *Model hypothesis and level of detail*

All glucose metabolism within the liver occurs in the hepatocytes, in a dynamic process that involves an exchange of substances between blood and cells. The hepatocyte is considered here as the elemental brick forming the sinusoid, therefore allowing the scaling-up of millions of sinusoids to represent the entire liver. The process/physiology analogy to develop the model is shown in Fig. 2. Blood entering the hepatic sinusoid gathers flows 1 and 2 (hepatic artery and portal vein, respectively). Here, blood volume and density are assumed to be constant due to the circulation's regulatory mechanisms that in usual conditions maintain strict control in human blood pressure, temperature, and density [35]. The hepatic sinusoid is considered a continuously stirred tank, and it is where the exchange of model's substances of interest takes place. The total amount of hepatocytes in a sinusoid is regarded as a two-zone continuous stirred tank reactor. In the upper part, it behaves like a regular continuously stirred reactor where all chemical reactions take place. In the lower part, it maintains perfect agitation and acts as a glycogen reservoir. The metabolic zonation of hepatic glucose metabolism [36] is not considered here since we aim at a net effect of the

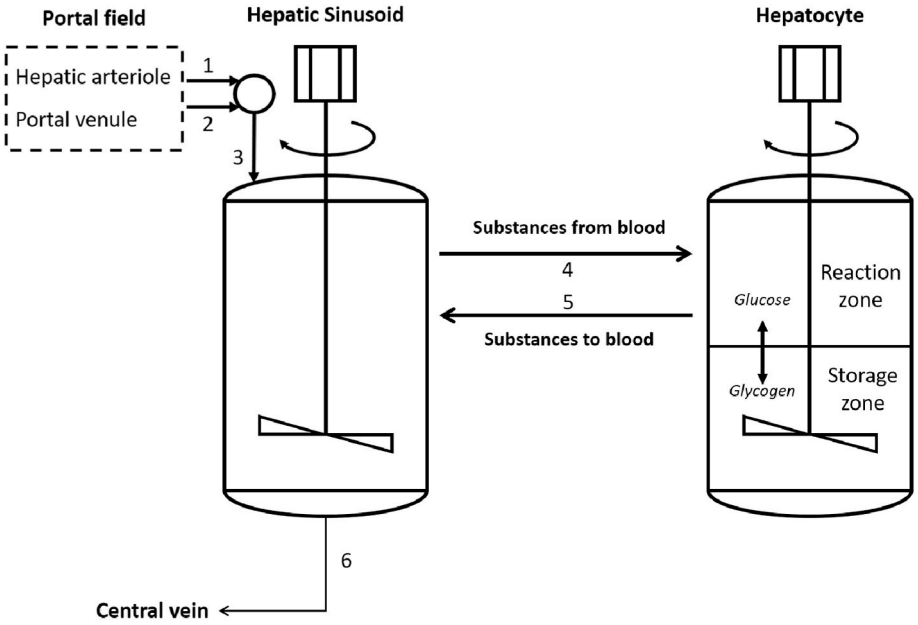

Fig. 2. Process/Physiology analogy used to build the mathematical model.

entire liver rather than a specific contribution from a given hepatocyte.

3.1.3. Definition of process systems (PS)

A Process System (PS) is an engineering abstraction of the real object allowing for the statement of a set of differential equations laying out the model's basic structure. Every PS is naturally a part of the modeled process, a volume where the properties of the substances of interest change [37]. Regarding the liver, three PSs were defined, see Fig. 3. PS_I is a mixing point merging the two blood streams entering the liver, the hepatic artery (stream 1) and portal vein (stream 2). The blood inflow to the hepatic sinusoids (PS_{III}) is hypothesized as a single flow represented by flow 3. We assume that all substances of interest, i.e., all substances playing a role in the glucose metabolism, diffuse across the blood vessels' walls irrigating the liver tissue to reach the hepatocytes (PS_{II}). This transport is represented with stream 4. Once in the hepatocytes, the necessary biochemical reactions take place and the products generated in these reactions return to the sinusoids via the mass flow 5, to be later discharged from PS_{III} to the bloodstream via stream 6.

3.2. Model construction

3.2.1. The conservation principle

Mass balances were applied in mass units to PS_I and PS_{III} for simplicity. We resorted to molar units in PS_{II} to handle all biochemical reactions of interest. Total mass balance and mass balance for each substance of interest were also formulated as shown below.

A. ***Hepatic sinusoid inlet*** (PS_I). All mass flows will be represented by $\dot{m}_k$, with k as the number or stream as in Fig. 3.

(i) *Total mass balance.* The total mass balance of PS_I is given by:

$$\frac{dM_I}{dt} = \dot{m}_1 + \dot{m}_2 - \dot{m}_3 \tag{1}$$

with M_I the total mass of substances contained in PS_I, $\dot{m}_1$ the oxygen-rich blood flow supply from the hepatic artery from the systemic circulation, and $\dot{m}_2$ the blood flow from the portal vein coming from the intestine with the absorbed nutrients. $\frac{dM_I}{dt} = 0$ given the constant blood volume and density. In this way, the total mass balance for the PS_I yields:

$$\dot{m}_3 = \dot{m}_1 + \dot{m}_2 \tag{2}$$

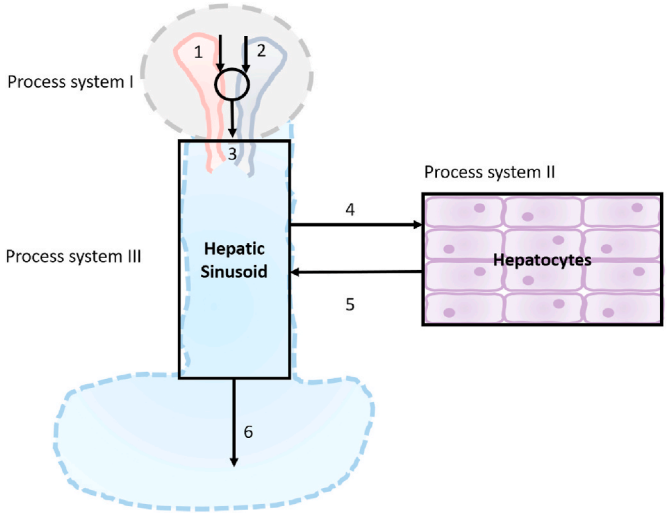

Fig. 3. Block diagram of process systems taken for modeling the liver's role in glucose metabolism. 1: Blood from the hepatic artery, 2: Blood from the portal vein, 3: Blood entering hepatic sinusoid, 4: Substances entering hepatocytes, 5: Substances leaving hepatocytes, 6: Blood to central hepatic vein.

(ii) *Component mass balance.* Glucose concentration from the splanchnic bed changes dynamically as per the mixing of the meal-related carbohydrate absorption and bloodstream coming from the systemic circulation. Essential hormones from the pancreas such as insulin and glucagon as well as non-carbohydrate gluconeogenesis precursors (i.e., lactate, glutamine, alanine, glycerol) are also included into the balances and generalized as

$$\frac{dM_{j,I}}{dt} = \dot{m}_1\, w_{j,1} + \dot{m}_2\, w_{j,2} - \dot{m}_3\, w_{j,3} \tag{3}$$

where $w_{j,k}$ is the mass fraction of component j in the stream k, with j: glucose (G), insulin (Ins), glucagon (Gluca), lactate (Lac), glutamine (Glut), alanine (Ala), and glycerol (Gly). Only amino acids from the systemic circulation are taken into account because amino acids from diet had little or no effect on hepatic glucose production [38]. Total mass of component j can be expressed as $M_{j,I} = w_{j,I} M_I$. Obtaining the derivative on this expression, considering perfect agitation ($w_{j,I} = w_{j,3}$) and $\frac{dM_I}{dt} = 0$ (total mass balance), Eq. (3) becomes

$$\frac{dw_{j,3}}{dt} = (\dot{m}_1\, w_{j,1} + \dot{m}_2\, w_{j,2} - \dot{m}_3\, w_{j,3})\frac{1}{M_I} \tag{4}$$

B. ***Hepatocytes*** (PS_{II}): In this PS, we consider the main biochemical reactions within the liver playing a role in glucose regulation. The liver keeps a similar EGP ratio from non-carbohydrate precursors in both postprandial and post-absorptive states. The stoichiometric balance for this glucose production is somehow equivalent to that occurring in the kidneys [11]. The remaining biochemical reactions present the following stoichiometric balances:

a. Glycogenesis ($i = 1$). The moles of glucose are phosphorylated to form moles of glycogen in the hepatocytes, with conversion of adenosine triphosphate (ATP) to adenosine diphosphate (ADP)

$$\text{Glucose - 1 - P} + \text{ATP} + \text{Glycogen}_n + H_2O \rightarrow \text{Glycogen}_{n+1} + \text{ADP} + 2\cdot\text{Pi}.$$

b. Glycogenolysis ($i = 2$). Glycogen dephosphorylates to form glucose

$$\text{Glycogen}_n + \text{Pi} \rightarrow \text{Glycogen}_{n-1} + \text{Glucose - 1 - P}.$$

c. Gluconeogenesis ($i = 3$). Stoichiometric balances via every non-carbohydrate precursor are reported elsewhere [11].

d. Insulin clearance and glucagon degradation ($i = 5$ and $i = 6$, respectively). These are equimolar reactions as follows

$$\text{Insulin} \rightarrow \text{Insulin*}\quad \text{Glucagon} \rightarrow \text{Glucagon*}$$

where Insulin* and Glucagon* are inactivated insulin and glucagon molecules, respectively.

e. Glycolysis ($i = 6$). Hepatocytes consume glucose at a constant rate during the postprandial state.

f. Lipogenesis ($i = 7$). Once glycogen stores in the liver reach their maximum capacity in the postprandial state, glucose is synthesized by an alternate metabolic pathway to form fat. This reaction also occurs during fasting when the hepatocytes catch half of the amount of glucose entering the sinusoid to form nicotine adenine dinucleotide phosphoric acid (NADPH). In both states, we consider an equimolar reaction as

$$\text{Glucose} \rightarrow G^*$$

with G^* being the fatty acids produced from glucose.

Fig. 4 summarizes the reactions taking into account in the model.

(i) *Total mass balance.* The total mass balance of the PS_{II} is written generically as

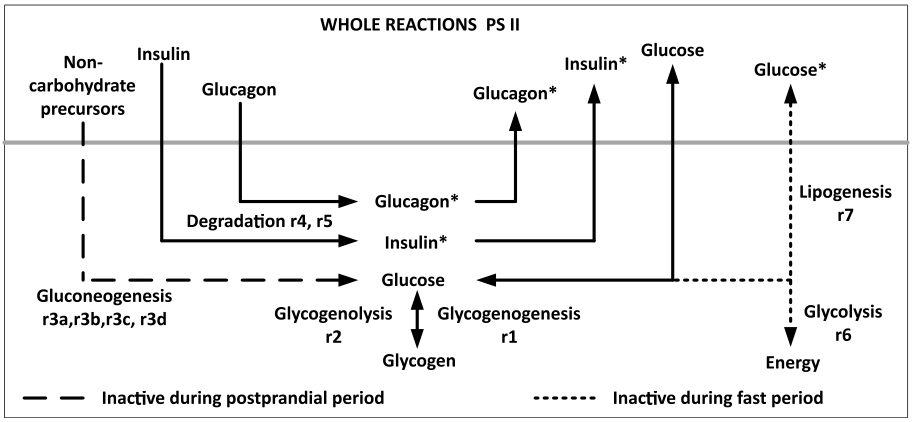

Fig. 4. Main biochemical reactions within the liver playing a role in glucose regulation.

$$\frac{dN_{II}}{dt} = \dot{n}_4 - \dot{n}_5 + \sum(r_i \sigma_{i,j}) \tag{5}$$

where N_{II} is the total mass of the substance in $kg - mol$. $\dot{n}_4$ is the molar flow of substance entering the hepatocytes in corresponding units. The amount of glucose from the blood in the sinusoids entering to the hepatocytes varies from around 50% in the fasting state to 30% after a meal [22]. In the fasting state, the liver prioritizes glucose consumption for energy production [22]. Most of the glucagon and insulin metabolism occurs in the liver; around 80% of the insulin and 58% of glucagon entering the liver undergo clearance in the hepatocytes [39,4, 40]. All the non-carbohydrate precursors for gluconeogenesis enter the reactor on. The products of the reactions in the hepatocytes are represented by $\dot{n}_5$ r_i is the reaction rate for glycolysis, glycogenesis, glycogenolysis, and gluconeogenesis, and also for insulin and glucagon inactivation. $\sigma_{i,j}$ represents the stoichiometric coefficients, with (+) sign for products and (−) sign for reactants. Subindices i and j represent the chemical reactions and reaction products, respectively. All insulin and glucagon that enters into the hepatocytes undergo proteolysis. Instead of including unnecessary additional balances, the model replaces the same amount of insulin and glucagon that enters through $\dot{n}_4$ into inactive products in $\dot{n}_5$, so there is no accumulation. Also, the model describes the liver clearance for both hormones with a positive sign (+) for products and a negative sign (−) for reactants.

(ii) *Component mass balance.* In this PS, glycogen also enters into play. Component mass balances for all species of interest in this PS can be written as

$$\frac{dN_{j,II}}{dt} = \dot{n}_4 x_{j,4} - \dot{n}_5 x_{j,5} + \sum(\sigma_{i,j} r_i) \tag{6}$$

with $N_{j,II}$ the total moles of every component of interest and $x_{j,5}$ the molar fraction of component j leaving the hepatocytes. For the sake of simplicity, the terms are written in molar flows of specific substance instead of molar fractions and total flows yielding

$$\frac{dN_{j,II}}{dt} = \dot{n}_{j,4} - \dot{n}_{j,5} + \sum(\sigma_{i,j} r_i) \tag{7}$$

where inactive glucose (G^*) produced via lipogenesis and Ins^* and $Gluca^*$ do not enter the hepatocytes since they are reaction products, therefore $\dot{n}_4 = 0$. The balance for G^*, Ins^*, and $Gluca^*$ might be rewritten as

$$\frac{dN_{j,II}}{dt} = -\dot{n}_{j,5} + \sum(\sigma_{i,j} r_i) \tag{8}$$

Once insulin, glucagon, and non-carbohydrates precursors enter the hepatocytes, they react and are converted into other substances not considered here. In this sense, $\dot{n}_{j,5} = 0$ and the mass balance for j = Ins, Gluca, Glut, Lac, Ala, and Gly becomes

$$\frac{dN_{j,II}}{dt} = \dot{n}_{j,4} + \sum(\sigma_{i,j} r_i) \tag{9}$$

Glycogen is phosphorylated and dephosphorylated only within the hepatocytes. Henceforth, there is no glycogen input/output. In this regard, the mass balance for glycogen is written as

$$\frac{dN_{j,II}}{dt} = \sum(\sigma_{i,j} r_i) \tag{10}$$

C. ***Hepatic sinusoid*** (PS_{III}). As mentioned earlier, for this PS balances are performed in mass units for simplicity.

(i) *Total mass balance.* Following the nomenclature in Fig. 3, the total mass balance for PS_{III} can be written as

$$\frac{dM_{III}}{dt} = \dot{m}_3 + \dot{m}_5 - \dot{m}_4 - \dot{m}_6 \tag{11}$$

In this PS there is no mass accumulation (blood density and volume remain constant), therefore $\frac{dM_{III}}{dt} = 0$ and

$$\dot{m}_6 = \dot{m}_3 + \dot{m}_5 - \dot{m}_4 \tag{12}$$

(ii) *Component mass balance.* In this PS, the focus is on in the species leaving the sinusoids via the hepatic vein. The component mass *balances* can be written in a general form as

$$\frac{dM_{j,III}}{dt} = \dot{m}_3 w_{j,3} + \dot{m}_5 w_{j,5} - \dot{m}_4 w_{j,4} - \dot{m}_6 w_{j,6} \tag{13}$$

with $M_{j,III}$ being the mass of component of interest j in the hepatic sinusoid. Using the perfect mixing condition of all substances into the hepatic sinusoid, the equivalence $w_{j,III} = w_{j,6}$ and $M_{j,III} = w_{j,III} M_{III}$ can be applied to solve the derivative of $M_{j,III}$, with M_{III} constant. Replacing this derivative solution in Eq. (13), the component mass balance in the PS_{III} becomes

$$\frac{dw_{j,6}}{dt} = (\dot{m}_3 w_{j,3} + \dot{m}_5 w_{j,5} - \dot{m}_4 w_{j,4} - \dot{m}_6 w_{j,6}) \frac{1}{\rho_b V_b} \tag{14}$$

in case $j = G$. With the above in mind, the mass balance for insulin, glucagon, and non-carbohydrates precursors yields

$$\frac{dw_{j,6}}{dt} = (\dot{m}_3 w_{j,3} - \dot{m}_4 w_{j,4} - \dot{m}_6 w_{j,6}) \frac{1}{\rho_b V_b} \tag{15}$$

For inactive insulin (Ins^*) and glucagon ($Gluca^*$) and fatty acids produced via lipogenesis (G^*), the balance reads as

$$\frac{dw_{j,6}}{dt} = (\dot{m}_5 w_{j,5} - \dot{m}_6 w_{j,6}) \frac{1}{\rho_b V_b} \tag{16}$$

3.2.2. The basic structure of the model

The basic structure of the model comes from the active balances detailed in the previous section. The equations with relevant information for each PS are described as follows.

- PS_I: Eqs. (3) and (5). The latter generates seven equations, one for every component *j*: glucose, insulin, glucagon, lactate, glutamine, alanine, and glycerol.
- PS_{II}: Eqs. (5) and (7) (for glucose), (8) (one for every inactive component j = *G**, *Ins**, and *Gluca**), (9) (for j = Ins, Gluca, Glut, Lac, Ala, and Gly), and (10) for glycogen.
- PS_{III}: Eqs. (12), (14) and (15) (for j = Ins, Gluca, Glut, Lac, Ala, Gly), (16) (one for every inactive component j = *Ins**, *Gluca**, and *G**).

In this sense, the basic structure of the model is composed of 31 equations as summarized in Table 1.

3.2.3. Variables, structural parameters, and structural constants

As detailed in Ref. [41], PBSMs is composed of variables, structural parameters, and constants. The structural parameters can be opened further to obtain a deeper level of detail. In the methodology used in this study [29], the parameters and constants that emerged from the application of the conservation principle are deemed as structural. While those that appear once the structural parameters have been defined are deemed as functional parameters. The classification of the model components are reported in Table 2.

3.2.4. Constitutive and assessment equations for structural and functional parameters. Definition of constants

As mentioned earlier, functional parameters show up once structural parameters are defined. The set of new equations proposed here to complete the whole structure of the model is labeled as an extended structure of the model. Mathematical expressions used to define a parameter in terms of new parameters are often known as constitutive equations. We use the term assessment equation to the assign a functional parameter with a given value either from the literature or from an assumption. Table 3 reports the set of constitutive equations used to define the structural parameters. In this table,"instances" refers to the number of equations generated given the different components of interest in that particular stream. Functional parameters can in turn be redefined in terms of new constitutive equations when deemed necessary. Table 4 details which functional parameters are re-defined. Finally, Table 5 summarizes all parameters with a fixed numerical value or defined by using an assessment equation as well as all model constants.

Table 1
Equations of the model's basic structure.

Process system	Equations	Component
PS_I	$\dot{m}_3 = \dot{m}_1 + \dot{m}_2$	
	$\frac{dw_{j,3}}{dt} = (\dot{m}_1 w_{j,1} + \dot{m}_2 w_{j,2} - \dot{m}_3 w_{j,3}) \frac{1}{\rho_b V_b}$	j = G, Ins, Gluca, Glut, Lac, Ala, Gly
PS_{II}	$\frac{dN_{II}}{dt} = \dot{n}_4 - \dot{n}_5 + \sum(r_i \sigma_{j,i})$	
	$\frac{dN_{j,II}}{dt} = \dot{n}_{j,4} - \dot{n}_5 x_{j,5} + \sum(r_i \sigma_{j,i})$	j = G
	$\frac{dN_{j,II}}{dt} = -\dot{n}_5 x_{j,5} + \sum(r_i \sigma_{j,i})$	j = *G**, *Ins**, *Gluca**
	$\frac{dN_{j,II}}{dt} = \dot{n}_{j,4} + \sum(r_i \sigma_{j,i})$	j = Ins, Gluca, Glut, Lac, Ala, Gly
	$\frac{dN_{j,II}}{dt} = \sum(r_i \sigma_{j,i})$	j = Glycogen
PS_{III}	$\dot{m}_6 = \dot{m}_3 + \dot{m}_5 - \dot{m}_4$	
	$\frac{dw_{j,6}}{dt} = (\dot{m}_3 w_{j,3} + \dot{m}_5 w_{j,5} - \dot{m}_4 w_{j,4} - \dot{m}_6 w_{j,6}) \frac{1}{\rho_b V_b}$	j = G
	$\frac{dw_{j,6}}{dt} = (\dot{m}_3 w_{j,3} - \dot{m}_4 w_{j,4} - \dot{m}_6 w_{j,6}) \frac{1}{\rho_b V_b}$	j = Ins, Gluca, Glut, Lac, Ala, Gly
	$\frac{dw_{j,6}}{dt} = (\dot{m}_5 w_{j,5} - \dot{m}_6 w_{j,6}) \frac{1}{\rho_b V_b}$	j = *G**, *Ins**, *Gluca**

The indexes are *j* = G, Ins, Gluca, Gluta, Lac, Ala, Gly, G*, Ins*, Gluca*, Glycogen; *i* (hepatic biochemical reactions): 1 = Glycogenesis, 2 = Glycogenolysis, 3 = Gluconeogenesis, 4 = Insulin clearance, 5 = Glucagon clearance, 6 = Glycolisis, 7 = Lipogenesis.

Table 2
Model variables, structural parameters, and structural constants.

	PS_I	PS_{II}	PS_{III}	Total
Variables	$\dot{m}_3, w_{j,3}$	N_{II}, $N_{j,II}$	$\dot{m}_6, w_{j,6}$	31
Structural Parameters	$\dot{m}_1, \dot{m}_2, w_{j,1}, w_{j,2}, \rho_b, V_b$	$\dot{n}_4, \dot{n}_5, \dot{n}_{j,4}, x_{j,5}, r_i$	$\dot{m}_4, \dot{m}_5, w_{j,4}, w_{j,5}$	42
Structural Constants	–	$\sigma_{j,i}$	–	26

The indexes are *j* = G, Ins, Gluca, Gluta, Lac, Ala, Gly, G*, Ins*, Gluca*, Glycogen; *i* (hepatic biochemical reactions): 1 = Glycogenesis, 2 = Glycogenolysis, 3 = Gluconeogenesis, 4 = Insulin clearance, 5 = Glucagon clearance, 6 = Glycolisis, 7 = Lipogenesis.

3.2.5. Analysis of degrees of freedom

The analysis of degrees of freedom in the model helps to establish the model closure in terms its computational solution. In this regard, our goal is to find whether the number of unknowns is equivalent to the number of equations (including variables and model parameters). For the purpose of the present model, we present the analysis of the degrees of freedom in Table 6, where a final 0 DoF is obtained. It is worth clarifying that the sole purpose of this analysis is to evaluate whether the model can be implemented in simulation. For identifiability purposes, the model can be parameterized with only twelve parameters. These tunable parameters must be defined by a numerical value that must be identified to provide a specific dynamic behavior.

3.3. Simulation of the computational model

3.3.1. Construction of the computational model

The model was programmed and solved using MatLab@ version 9.8.0 - R2020a (Natick, Massachusetts: The MathWorks Inc.).

3.3.2. Model validation

In this initial stage, we contrasted the model response with experimental data found from three different in-vivo experiments [13,14,15]. Further details will be presented in the Results Section.

4. Results

We presented a detailed Phenomenological-Based Semi-physical Models (PBSM) of the human hepatic glucose metabolism for healthy subjects accounting for the two major hormones involved in glucose regulation, insulin and glucagon. Results from three different experiments available in the literature were used to assess the prediction ability of the proposed model [13,14,15]. It is worth mentioning that since the three experimental conditions are different, the types of stimuli and observations also differ from one another. In this case, since we are interested in assessing the physiological coherence of the model, we replicated at replicating the median traces of the experimental outputs by considering a hypothetical "median" virtual subject.

Fig. 5 shows the results of our model in reconstructing the experimental results presented in Ref. [15], where 11 subjects underwent an Oral Glucose Tolerance Test (OGTT) following an overnight fast. The purpose of the experiment was to measure the rate of oral glucose appearance, splanchnic glucose uptake, suppression of hepatic glucose production, and peripheral glucose uptake using hepatic vein

Table 3
Constitutive equations for structural parameters of the model.

#	Description	Constitutive/Assessment Equation	Instances	Ref.
1	Mass flow rate of blood entering in the liver from the hepatic artery (stream 1).	$\dot{m}_1 = \rho_b \dot{V}_{ab}$	1	[42]
2	Mass flow rate of blood entering in the liver from the portal vein (stream 2).	$\dot{m}_2 = \rho_b \dot{V}_{vb}$	1	[42]
3	Mass fraction of components of interest entering in the liver via the hepatic artery.	$w_{j,1} = C_{j,1} \frac{1}{\rho_b} \mathfrak{M}_j$	7	UC
4	Mass fraction of components of interest entering in the liver via the portal vein.	$w_{j,2} = C_{j,2} \frac{1}{\rho_b} \mathfrak{M}_j$	7	UC
5	Density of the blood.	$\rho_b = 1060\ \mathrm{kg/m^3}$	1	[43]
6	Volume of blood irrigating the liver.	$V_b = 0.25\ vol$	1	
7	Molar flow of substances of interest involved in glucose metabolism entering hepatocytes from sinusoids.	$\dot{n}_4 = \sum \dot{n}_{j,4}$	1	[42]
8	Molar flow of substances of interest out of the hepatocytes towards the sinusoids	$\dot{n}_5 = \dot{V}_5 \overline{\rho}_5$	1	[42]
9	Reaction velocity of insulin and glucagon clearance, and gluconeogenesis occurring in the liver.	$r_i = k_{0,i} N_{j,II} e^{\frac{-Ea_i}{RT}}$	3	[42]
10	Rate of glycogenogenesis reaction occurring in the liver in both postprandial and postabsorptive states.	$r_1 =$	1	[44, 45]
11	Rate of glucose production from glycogen stored in the liver.	$\begin{cases} 0 & \text{if } C_{G,2} \le C_{G,1} \wedge N_{Glgn,II} > 500\ mol \\ k_{0,1} x_{G,4} e^{\frac{-Ea_1}{RT}} & \text{if } C_{G,2} > C_{G,1} \end{cases}$	1	[44, 45]
		$r_2 = \begin{cases} k_{0,2} N_{Glgn,II} e^{\frac{-Ea_2}{RT}} & \text{if } C_{G,2} \le C_{G,1} \wedge C_{Gluca} > 77\ pmol/L \wedge N_{Glgn,II} > N_{Glgn,II_{min}} \\ 0 & \text{if } C_{G,2} > C_{G,1} \vee N_{Glgn,II} \le N_{Glgn,II_{min}} \wedge C_{Gluca} > 77\ pmol/L \wedge C_{G,2} \le C_{G,1} \end{cases}$		
12	Rate of glucose consumption by hepatocytes (glycolysis).	$r_6 = \begin{cases} 0 & \text{if } C_{G,2} \le C_{G,1} \\ k_{0,6} x_{G,4} e^{\frac{-Ea_6}{RT}} & \text{if } C_{G,2} > C_{G,1} \end{cases}$	1	[46]
13	Fat production rate by lipogenesis due to excess glucose in the liver.	$r_7 = \begin{cases} k_{0,7} x_{G,4} e^{\frac{-Ea_7}{RT}} & \text{if } C_{G,2} \le C_{G,1} \\ 0 & \text{if } C_{G,2} > C_{G,1} \wedge N_{Glgn,II} \le 500\ \mu mol \\ k_{0,7} N_{G,II} e^{\frac{-Ea_7}{RT}} & \text{if } C_{G,2} > C_{G,1} \wedge N_{Glgn,II} > 500\ \mu mol \end{cases}$	1	[44, 45]
14	Molar flow of glucose entering the hepatocytes.	$\dot{n}_{G,4} = \begin{cases} PU_{G_{pv}} \dot{n}_{G,3} & \text{if } C_{G,2} \le C_{G,1} \\ PU_{G_{pp}} \dot{n}_{G,3} & \text{if } C_{G,2} > C_{G,1} \end{cases}$	1	A
15	Molar flow of insulin entering the hepatocytes.	$\dot{n}_{Ins,4} = PC_{Ins} \dot{n}_{Ins,3}$	1	[47]
16	Molar flow of glucagon entering the hepatocytes.	$\dot{n}_{Gluca,4} = PC_{Gluca} \dot{n}_{Gluca,3}$	1	A
17	Molar flow of non-carbohydrate precursor entering the hepatocytes.	$\dot{n}_{j,4} = C_{j,3} \dot{V}_{hep} PC_j$	4	[44]
18	Molar fraction of glucose (G), inactive glucose (G^*), inactive insulin (Ins^*), and inactive glucagon ($Gluca^*$) leaving the hepatocytes.	$x_{j,5} = \frac{N_{j,II}}{N_{II}}$	4	[42]
19	Mass flow rate of substances of interest entering the hepatocytes.	$\dot{m}_4 = \sum(\dot{n}_4 \mathfrak{M}_j)$	1	UC
20	Mass flow rate of the reaction products returning to the bloodstream from the hepatocytes.	$\dot{m}_5 = \dot{n}_5 \mathfrak{M}_5$	1	UC
21	Mass fraction of component j entering the hepatocytes by stream 4.	$w_{j,4} = \dot{n}_{j,4} \mathfrak{M}_j \frac{1}{\dot{m}_4}$	7	UC
22	Mass fraction of component j leaving the hepatocytes by stream 5.	$w_{j,5} = x_{j,5} \frac{\mathfrak{M}_j}{\mathfrak{M}_5}$	10	UC

Abbreviations. UC: Unit conversion, A: Assumed. Indexes j = G, Ins, Gluca, Gluta, Lac, Ala, Gly, G^*, Ins^*, $Gluca^*$, Glgn. Indexes i (biochemical reactions): 1 = Glucogenogenesis, 2 = glycogenolysis, 3 = Gluconeogenesis, 4 = Insulin clearance, 5 = Glucagon clearance, 6 = Glycolysis, 7 = Lipogenesis.

catheterization and a double-tracer technique. For the considered scenario, absolute errors of (mean ± std) 5.4 ± 5.2 mg/dL, 38.7 ± 28.4 *pmol/L*, and 41.1 ± 101.6 μmol were obtained for systemic glucose, systemic insulin, and glycogen, respectively, when comparing the model output with respect to the available experimental data.

Fig. 6 shows the results of the developed model in reproducing the experimental setup in Ref. [14], where 88 healthy subjects (46 male - 42 female) underwent an OGTT. The rate of glucose appearance was estimated from a two-tracer protocol. For the considered scenario, absolute errors of (mean ± std) 7.5 ± 6.8 mg/dL and 15.3 ± 15.4 *pmol/L* were obtained for systemic glucose and systemic insulin, respectively, when comparing the model output with respect to the available experimental data.

A more realistic setup where 16 healthy subjects were challenged with a mixed meal after overnight fasting was considered by Basu et al. in Ref. [13]. This experiment provided information following a more conventional meal and reports useful information such as the rate of glucose appearance (Ra) and C-peptide concentration, estimated by means of a triple-tracer technique, allowing the estimation of pancreatic insulin within the portal vein after the meals. Fig. 7 shows the performance of our model in reproducing such results. Absolute errors of (mean ± std) 7.5 ± 7.5 mg/dL, 30.9 ± 48.5 *pmol/L*, and 0.49 ± 0.45 *pmol/L* were obtained for systemic glucose, systemic insulin, and systemic glucagon, respectively, when comparing the model output with respect to the available experimental data.

Table 4
Constitutive equations for functional parameters of the model.

#	Description	Constit. Equation	Instances	Ref.
1	Volumetric flow rate of blood entering the liver from the hepatic artery.	$\dot{V}_{ab} = 10\ \frac{mL}{kg-min}$	1	[48]
2	Volumetric flow rate of blood entering the liver from the portal system.	$\dot{V}_{vb} = 20\ \frac{mL}{kg-min}$	1	[48]
3	Circulating blood volume.	$Vol = 80$ BW	1	[48]
4	Volumetric flow rate out of hepatocytes.	$\dot{V}_5 = \sum(\dot{V}_{r_i}) + \sum(\dot{V}_4)$	1	O
5	Average molar density of flow out of hepatocytes (stream 5).	$\overline{\rho}_5 = \frac{1}{\sum\frac{x_{j,5}}{\overline{\rho}_j}}$	1	O
6	Molar fraction of component j entering the hepatocytes.	$x_{j,4} = \frac{\dot{n}_{j,4}}{\dot{n}_4}$	3	UC
7	Molar flow of $j = G$, *Ins*, and *Gluca* entering the hepatic sinusoids via stream 3.	$\dot{n}_{j,3} = w_{j,3}\ \frac{1}{\mathfrak{M}_j}\ \dot{m}_3$	3	UC
8	Molar-volumetric concentration of component $j = G$, *Ins*, and *Gluca* entering the hepatic sinusoids.	$C_{j,3} = w_{j,3}\ \rho_b\ \frac{1}{\mathfrak{M}_j}$	3	UC
9	Volumetric flow entering the hepatocytes.	$\dot{V}_{hep} = 0.6\ \dot{V}_b$	1	[48]
10	Total molar mass of components leaving liver and returning the hepatic sinusoids via stream 5	$\mathfrak{M}_5 = \sum(x_{j,5}\ \mathfrak{M}_j)$	1	[42]
11	Volumetric flow due to reaction i.	$\dot{V}_{r_i} = \sigma_{G,i}\ r_i\ \frac{1}{\overline{\rho}_G}$	3	A
12	Volumetric flow in the stream 4.	$\dot{V}_4 = \dot{n}_4\ \frac{1}{\overline{\rho}_4}$	1	A
13	Total volumetric flow of blood entering the liver.	$\dot{V}_b = \dot{V}_{ab} + \dot{V}_{vb}$	1	O
14	Average molar density of stream 4 that enters the hepatocytes.	$\overline{\rho}_4 = \frac{1}{\sum(\frac{x_{j,4}}{\overline{\rho}_j})}$	1	O
15	Molar flow of stream 4.	$\dot{n}_4 = \sum(\dot{n}_{j,4})$	1	[42]

Abbreviations. O: Own equation. UC: Unit conversion, A: Assumed. Indexes $j =$ G, Ins, Gluca, Gluta, Lac, Ala, Gly, *G**, *Ins**, *Gluca**, Glgn. Indexes i (biochemical reactions): 1 = Glucogenogenesis, 2 = glycogenolysis, 3 = Gluconeogenesis, 4 = Insulin clearance, 5 = Glucagon clearance, 6 = Glycolysis, 7 = Lipogenesis.

5. Discussion

This work presents a phenomenological-based model describing the flows of glucose, insulin, and glucagon in both fasting and postprandial states in non-diabetic individuals and the changes in liver glycogen concentrations. The simulation results showed the model's ability in reproducing results from several experimental setups involving different measurement methods, stimuli, and measured variables. Despite the crucial role that the liver plays in glucose metabolism, most mathematical models available in the literature have typically described parts of that role through compartmental models (either minimal or maximal).

Single-compartment models have shown limitations in recreating hepatic glucose production, especially in the non-steady state. Two-compartment models were developed to describe this dynamic during an intravenous glucose tolerance test (IVGTT) [53]. Although minimal models are parsimonious, the simplistic mathematical structure makes them prone to averaging the data instead of providing an actual explanation for the experiment. Moreover, in spite of the involvement of certain physiological knowledge (arguably, compartmental modeling is usually built upon strong assumptions to keep the model structure simple), its extension to slightly different conditions is usually not straightforward. The Sorensen model [54] is one of the most complex physiological compartmental models used to describe whole body glucose homeostasis. In the model, two different compartments

Table 5
Assessment equations for functional parameters of the model. The numerical values are fixed parameters in the model. Constants of the model are also reported in this table shown in the "value" column.

Symbol	Description	Value	Instances	Ref.
$C_{j,1}$	Molar-volumetric concentration of component j in systemic circulation entering the liver via stream 1.	Experimental data was considered for $j = G$ and *Ins*.	2	[13, 15]
$C_{Gluca,1}$	Molar-volumetric concentration of glucagon in systemic circulation entering the liver via stream 1.	Experimental data was considered for $j =$ *Gluca* when information was available. Otherwise, a concentration of 100 *pmol/L* was considered.	1	[44]
$C_{Gluta,1}$	Molar-volumetric concentration of glutamine in systemic circulation entering the liver via stream 1.	0.6 mmol/L	1	[49]
$C_{Lac,1}$	Molar-volumetric concentration of lactate in systemic circulation entering the liver via stream 1.	0.8 mmol/L	1	[49]
$C_{Ala,1}$	Molar-volumetric concentration of alanine in systemic circulation entering the liver via stream 1.	0.3 mmol/L	1	[49]
$C_{Gly,1}$	Molar-volumetric concentration of gly in systemic circulation entering the liver via stream 1.	0.1 mmol/L	1	[49]
$C_{j,2}$	Molar-volumetric concentration of component j in portal venous system entering the liver via stream 2.	Experimental data was considered for $j = G$, *Ins*, and *Gluca*. For $j =$ precursors, concentrations are considered the same values of $C_{j,1}$	3	[13, 14, 15]
$\mathfrak{M}_j$	Molar mass of component j (known value).		7	A
$k_{0,i}$	Theconstant rate of glucose production and consumption due to biochemical reactions involved in glucose metabolism and that take place in the liver.		7	I
Ea_i	Activation energy for glucose production and consumption via biochemical reactions involved in glucose metabolism and taking place in the liver.		7	I
$PU_{G,pa}$	Percentage of glucose uptake in the liver in post-absorptive state.	50%	1	[20]
$PU_{G,pp}$	Percentage of glucose uptake in the liver in postprandial state.	21%	1	[20]
PC_{Ins}	Percentage of insulin clearance in the liver.	71%. Range reported in the literature 20–80%	1	I
PC_{Gluca}	Percentage of glucagon clearance in the liver.	58%	1	A
PC_j	Uptake percentage of non-carbohydrate precursors in the liver.		4	I

(*continued on next page*)

Table 5 (*continued*)

Symbol	Description	Value	Instances	Ref.
BW	Body weight.	70 kg	1	A
$\overline{\rho}_j$	Molar density of component j.		4	A
R	Universal constant for ideal gas.	8.314 J/molK	1	[42]
T	Blood temperature.	37 °C	1	[50]
$\sigma_{j,i}$	Stoichiometric coefficient for component j in the reaction i where is consumed.	−1	6	[51, 52, 52]
$\sigma_{j,i}$	Stoichiometric coefficient for component j in the reaction i where is produced.	1	5	[51, 52, 52]

Abbreviations. A: Assumed. I: Identified. Indexes j = G, Ins, Gluca, Gluta, Lac, Ala, Gly, G*, *Ins**, *Gluca**, Glgn. Indexes i (biochemical reactions): 1 = Glucogenogenesis, 2 = glycogenolysis, 3 = Gluconeogenesis, 4 = Insulin clearance, 5 = Glucagon clearance, 6 = Glycolysis, 7 = Lipogenesis.

Table 6
Degrees of freedom.

	V	SP	FP	Net	DoF
Equations	31	23	57	111	0
Unknowns	31	23	57	111	

Abbreviations. V: variables, SP: structural parameters, FP: functional parameters, Net: sum of $SP + FP + V$, and DoF: degrees of freedom (difference between unknowns and equations).

represent glucose and insulin metabolism. However, the liver's role is simplified to a mass balance equation preventing the model from obtaining estimations of other hepatic processes such as hepatic glucose production.

In [55], the authors developed a maximal compartmental model to describe the so-called glucose-insulin system after a glucose load in both healthy subjects and those with T2D. This model version, which later gave way to the well-known UVA-Padova simulator did not include the glucagon action. In this model, the glucose liver's glucose production is presented in terms of glucose and insulin signals. Several parameters need to be identified from multiple tracer experiments, such as the effectiveness of liver glucose effectiveness, amplitude of the action of insulin on the liver, amplitude of the action of the portal insulin on the liver, and the delay between insulin signal and insulin action. Hepatic insulin metabolism is also incorporated through two clearance terms involving the portal insulin secreted by the pancreas and a more difficult to interpret "delayed" insulin signal I_d. The role of glucagon and the use of the simulation model in subjects with T1D is included in Ref. [56].

In spite of the considerable effort to obtain a model of first principles, we ended up with a highly descriptive model with parameter interpretability and few parameters to calibrate (individualize). As shown in Figs. 5–7, the predictions made for a virtual averaged subject coincide with the observed behavior in three different, unrelated experiments.

Other compartmental models involving different aspects of the hepatic glucose metabolism can be found elsewhere [57], or using data related to pharmacokinetics/pharmacodynamics rather than experiments made under physiological conditions [58]. Chalhoub et al. proposed a model for the key reactions of carbohydrates metabolism and transport in the liver [57]. This model was built with information from previous models and intended to explain carbohydrate metabolism changes related to high-intensity exercise. In addition, this model recreates hepatocytes zonation, a characteristic not included in our model as we were interested in the net effect of the entire liver. The ability of our model to reproduce data from an experiment that measured glucose concentration in the hepatic vein [15] suggests that liver metabolic zonation can be simplified if the modeling objective is the contribution of the entire organ in the glucose metabolism.

Mathematical models can also be used to explain the kinetics of the reactions that take place in glucose metabolism. Glycogen synthesis and degradation are essential for gluconeogenesis. El-Refai [59] and collaborators proposed a detailed six-compartmental model to explain glycogen formation from glucose and vice-versa using plasma glucose concentration, liver glycogen level, and a chemical reaction rate. The model made it possible to describe different liver-related insulin actions to glucose metabolism and carbon incorporation to the glycogen formation cycle via simulation. Fig. 5 shows how our model can recreate the liver's glycogen formation after a meal using stoichiometric balances. This information can determine the glucose production rate via glycogenolysis during the fasting state, allowing more extended simulations to be performed.

Mechanistic detailed models like the proposed here can be used to obtain clinically meaningful information. One of the most detailed models for the role played by the liver in glucose metabolism was proposed by König and collaborators. It made it possible to simulate liver carbohydrate metabolism at the molecular level with hormonal regulation [44]. This "stand-alone" liver model was then used to explain the possible mechanisms behind the augmented hypoglycemia risk seen in patients with type 2 diabetes mellitus under insulin treatment [60]. As with König's model, our model agrees with the experimental data from the liver's internal process, including the hepatic glucose production, hepatic glucose utilization, and hormonal control, and it recreates both postprandial and fasting states. Unfortunately, to the best of the authors knowledge, a detailed explanation of the set of differential equations is currently unavailable which hampers further comparisons.

Extended models can theoretically have a better predictive ability as they incorporate more physiological information. The proposed model can be integrated with additional models via the circulation to form a digital copy of the human glucose metabolism. Further investigation will be needed to reach a the level of progress of currently available simulation models [55,61,62,56]. However, in these models, the role of the liver in glucose homeostasis has been simplified to the main functions of glucose uptake and production with less consideration to hormonal and metabolic modulation of these processes; some of these models even consider a constant rate of glucose production. Our model incorporates both hormonal and metabolic modulation in glucose production and uptake, leading to a more precise recreation of the liver's role in glucose homeostasis.

6. Conclusion

The liver plays an important role in glucose regulation in the human body, but its physiological aspects have been reduced in the existing mathematical models for simplicity. A phenomenological-based model able to reproduce not only the key metabolic pathways but also the complex hormonal regulation can have several applications, for example, in the study the physiology in healthy and non healthy subjects, as well as in the development of therapeutic interventions for people with diabetes. The methodological approach proposed in this work allows having parameters interpretability resulting in an easy way to adjust the kinetics parameters of the model. It is also versatile due to its basic structure allowing its adaptation to different conditions. Perhaps the only limitation of the model is the large number of parameters, which makes it difficult to implement in some practices. Finally, this model could be combined with other models to form a whole-body glucose metabolism model.

Funding sources

L. Lema-Perez was funded by a doctoral scholarship from the Administrative Department of Science, Technology, and Innovation of

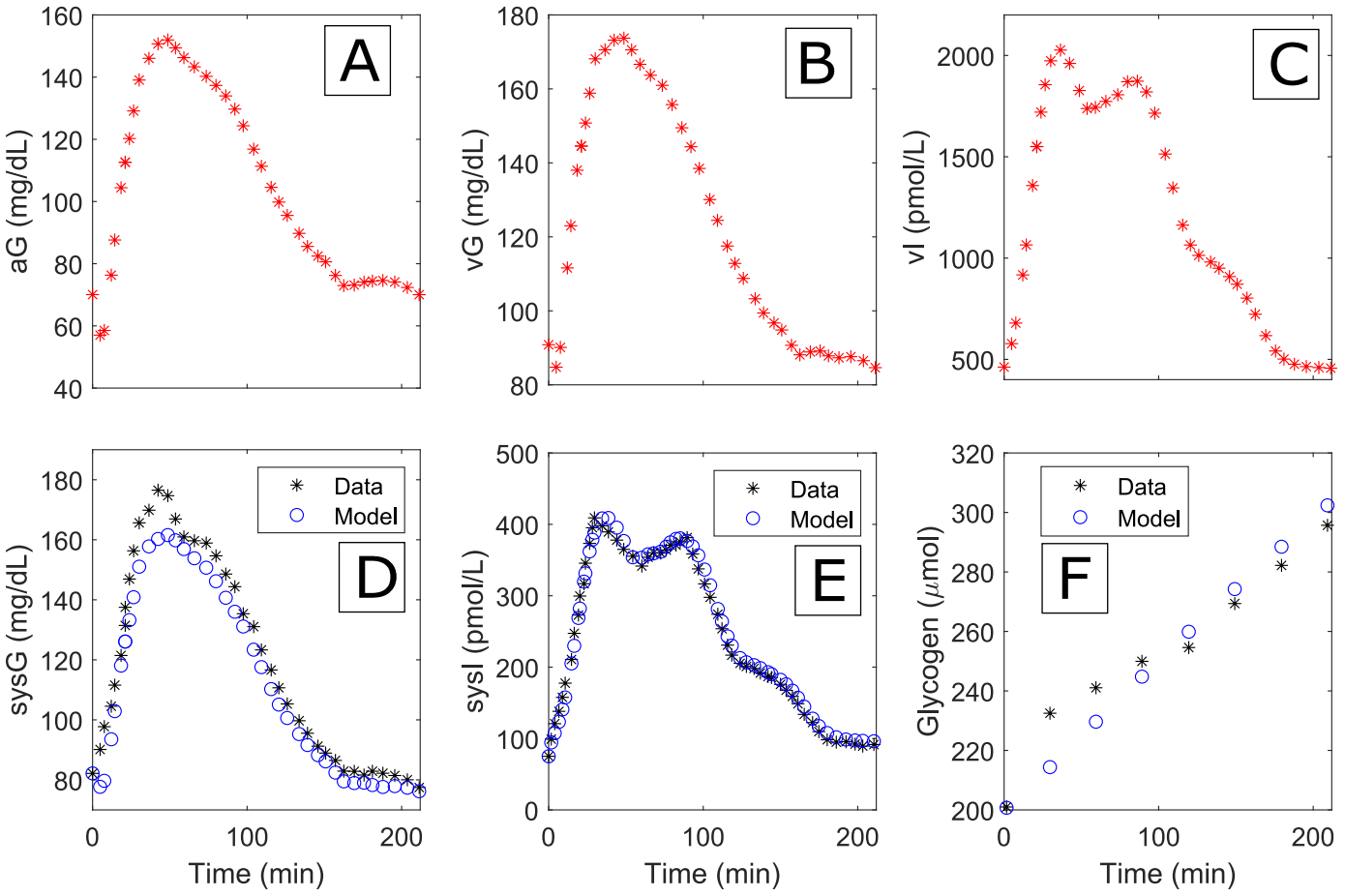

Fig. 5. Panels A–C represent the inputs: (A) arterial glucose concentration (aG), (B) venous glucose concentration (vG), and (C) venous insulin concentration (vI). Panels D–F depict the model outputs: (D) systemic glucose (sysG), (E) systemic insulin (sysI), and (F) Glycogen.

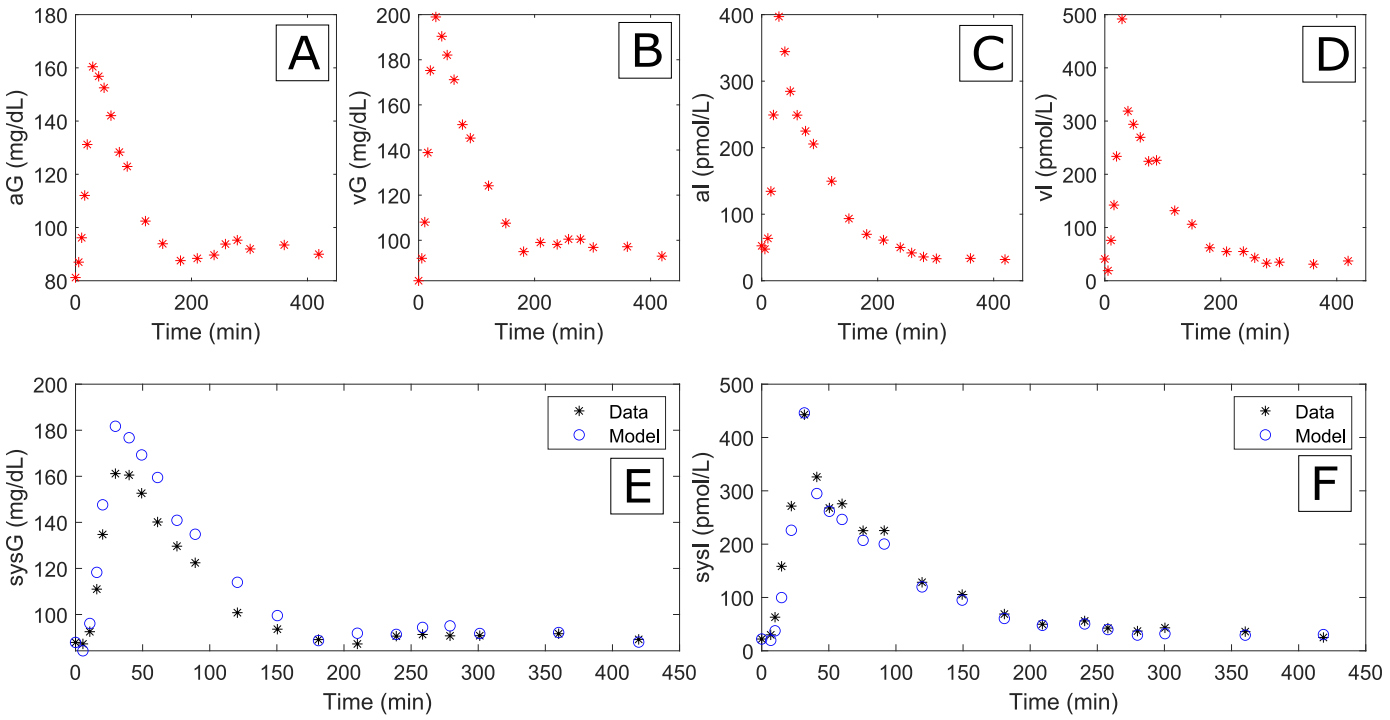

Fig. 6. Panels A–D represent the inputs: (A) arterial glucose concentration (aG), (B) venous glucose concentration (vG), (C), arterial insulin concentration (aI) and (D) venous insulin concentration (vI). Panels E–F depict the model outputs: (E) systemic glucose (sysG) and (F) systemic insulin (sysI).

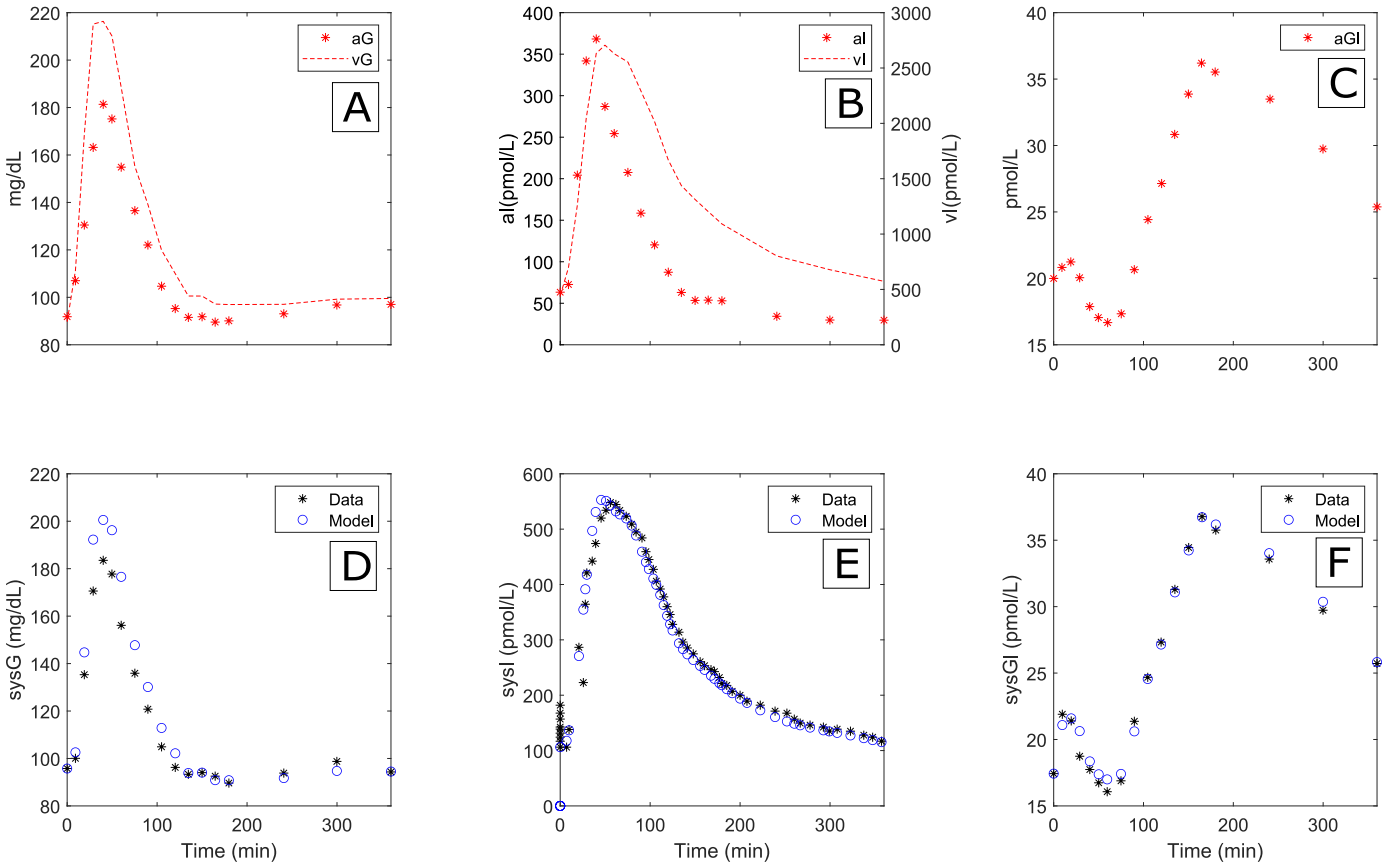

Fig. 7. Panels A–C represent the inputs: (A) arterial and venous glucose concentration (aG, vG), (B) arterial and venous insulin concentration (aI, vI), and (C) arterial glucagon concentration (aGl). Panels D–F depict the model outputs: (D) systemic glucose (sysG) and (E) systemic insulin (sysI), and (F) systemic Glucagon.

Colombia - Colciencias.

Declaration of competing interest

Laura Lema-Perez and Hernan Alvarez certify that they have no affiliation or involvement with any organization or entity with any financial (fees, financial aid for education, shares, employment contracts, work as consultants, or any other type of interest) or non-financial interest (personal or professional relationships, affiliations, or beliefs) in the topic of interest or any material discussed in this manuscript. Carlos E. Builes-Montaño has received consulting or speaker fees from Sanofi, Novo Nordisk, Novartis, and Boehringer Ingelheim. Jose Garcia-Tirado reports receiving industry research support and royalties from Dexcom through his institution.

References

[1] R.N. Bergman, F. Piccinini, M. Kabir, M. Ader, Novel aspects of the role of the liver in carbohydrate metabolism, Metab. Clin. Exp. 99 (2019) 119–125.
[2] R.S. Sherwin, Role of liver in glucose homeostasis, Diabetes Care 3 (1980) 261–265.
[3] M.C. Laurenti, A. Vella, J.D. Adams, D.J. Schembri Wismayer, A.M. Egan, C. Dalla Man, Assessment of individual and standardized glucagon kinetics in healthy humans, Am. J. Physiol. Endocrinol. Metabol. 320 (2021) E71–E77.
[4] S.M. Najjar, G. Perdomo, Hepatic insulin clearance: mechanism and physiology, Physiology 34 (2019) 198–215.
[5] S. Gorban, A. Ferreira de Moura, C. Decroux, L. Duke, L. Hammond, et al., IDF Diabetes Atlas, ninth ed., International Diabetes Federation, 2019.
[6] American Diabetes Association, Diabetes technology: standards of medical care in diabetes—2020, Diabetes Care 43 (2020) S77–S88.
[7] N. Kaufman, Digital therapeutics: leading the way to improved outcomes for people with diabetes, Diabetes Spectr. 32 (2019) 301–303.
[8] B. Kovatchev, A century of diabetes technology: signals, models, and artificial pancreas control, Trends Endocrinol. Metabol. 30 (2019) 432–444.
[9] B.P. Kovatchev, M. Breton, C. Dalla Man, C. Cobelli, In silico preclinical trials: a proof of concept in closed-loop control of type 1 diabetes, J. Diabetes.Sci. Technol. 3 (2009) 44–55.
[10] C. Cobelli, C. Dalla Man, G. Sparacino, L. Magni, G. De Nicolao, B.P. Kovatchev, Diabetes: models, signals, and control, IEEE. Rev. Biomed. Eng. 2 (2009) 54–96.
[11] L. Lema-Perez, C.E. Builes-Montaño, H. Alvarez, A phenomenological-based semi-physical model of the kidneys and its role in glucose metabolism, J. Theor. Biol. 508 (2020) 110489.
[12] L. Lema-Perez, J. Garcia-Tirado, C. Builes-Montaño, H. Alvarez, Phenomenological-based model of human stomach and its role in glucose metabolism, J. Theor. Biol. 460 (2019) 88–100.
[13] R. Basu, M. Schiavon, X.M. Petterson, L. Hinshaw, M. Slama, R. Carter, C.D. Man, C. Cobelli, A. Basu, A novel natural tracer method to measure complex carbohydrate metabolism, Am. J. Physiol. Endocrinol. Metabol. 317 (2019) E483–E493.
[14] C. Dalla Man, A. Caumo, R. Basu, R. Rizza, G. Toffolo, C. Cobelli, Minimal model estimation of glucose absorption and insulin sensitivity from oral test: validation with a tracer method, Am. J. Physiol. Endocrinol. Metabol. 287 (2004) E637–E643.
[15] E. Ferrannini, O. Bjorkman, G.A. Reichard, A. Pilo, M. Olsson, J. Wahren, R. A. DeFronzo, The disposal of an oral glucose load in healthy subjects: a quantitative study, Diabetes 34 (1985) 580–588.
[16] J. Radziuk, Tracer methods and the metabolic disposal of a carbohydrate load in man, Diabetes Metab. Rev. 3 (1987) 231–267.
[17] A. Adkins, R. Basu, M. Persson, B. Dicke, P. Shah, A. Vella, W.F. Schwenk, R. Rizza, Higher insulin concentrations are required to suppress gluconeogenesis than glycogenolysis in nondiabetic humans, Diabetes 52 (2003) 2213–2220.
[18] H.S. Han, G. Kang, J.S. Kim, B.H. Choi, S.H. Koo, Regulation of glucose metabolism from a liver-centric perspective, Exp. Mol. Med. 48 (2016) e218–e218.
[19] K.J. Ahn, J.S. Kim, M.J. Yun, J.H. Park, J.D. Lee, Enzymatic properties of the n-and c-terminal halves of human hexokinase ii, BMB reports 42 (2009) 350–355.
[20] H.J. Woerle, C. Meyer, J.M. Dostou, N.R. Gosmanov, N. Islam, E. Popa, S. D. Wittlin, S.L. Welle, J.E. Gerich, Pathways for glucose disposal after meal ingestion in humans, Am. J. Physiol. Endocrinol. Metabol. 284 (2003) E716–E725.
[21] R.M. McDevitt, S.J. Bott, M. Harding, W.A. Coward, L.J. Bluck, A.M. Prentice, De novo lipogenesis during controlled overfeeding with sucrose or glucose in lean and obese women, Am. J. Clin. Nutr. 74 (2001) 737–746.
[22] J. Radziuk, S. Pye, Hepatic glucose uptake, gluconeogenesis and the regulation of glycogen synthesis, Diabetes.Metabol. Res. Rev. 17 (2001) 250–272.
[23] A. Vandercammen, E. Van Schaftingen, Competitive inhibition of liver glucokinase by its regulatory protein, Eur. J. Biochem. 200 (1991) 545–551.

[24] P. Iynedjian, D. Jotterand, T. Nouspikel, M. Asfari, P. Pilot, Transcriptional induction of glucokinase gene by insulin in cultured liver cells and its repression by the glucagon-camp system, J. Biol. Chem. 264 (1989) 21824–21829.
[25] K.S. Brown, S.S. Kalinowski, J.R. Megill, S.K. Durham, K.A. Mookhtiar, Glucokinase regulatory protein may interact with glucokinase in the hepatocyte nucleus, Diabetes 46 (1997) 179–186.
[26] D. Argaud, Q. Zhang, W. Pan, S. Maitra, S.J. Pilkis, A.J. Lange, Regulation of rat liver glucose-6-phosphatase gene expression in different nutritional and hormonal states: gene structure and 5′-flanking sequence, Diabetes 45 (1996) 1563–1571.
[27] D. Massillon, N. Barzilai, W. Chen, M. Hu, L. Rossetti, Glucose regulates in vivo glucose-6-phosphatase gene expression in the liver of diabetic rats, J. Biol. Chem. 271 (1996) 9871–9874.
[28] D. Massillon, M. Bollen, H. De Wulf, K. Overloop, F. Vanstapel, P. Van Hecke, W. Stalmans, Demonstration of a glycogen/glucose 1-phosphate cycle in hepatocytes from fasted rats selective inactivation of phosphorylase by 2-deoxy-2-fluoro-α-d-glucopyranosyl fluoride, J. Biol. Chem. 270 (1995) 19351–19356.
[29] R. Lamanna, P. Vega, S. Revollar, H. Alvarez, Diseño Simultáneo de Proceso y Control de una Torre Sulfitadora de Jugo de Caña de Azúcar, Revista Iberoamericana de Automática e Informática Industrial RIAI 6 (2009) 32–43.
[30] D. Arbelaez-Gomez, S. Benavides-Lopez, M.P. Giraldo-Agudelo, J.P. Guzman-Alvarez, C. Ramirez-Mazo, L.M. Gomez-Echavarria, A phenomenological-based model of the endometrial growth and shedding during the menstrual cycle, J. Theor. Biol. 532 (2021) 110922.
[31] A. Herron-Bedoya, M. Walteros-Leon, L. Lema-Perez, H. Alvarez, Phenomenological-based model of glucose transport from liver to abdominal subcutaneous adipose tissue, J. Theor. Biol. 530 (2021) 110883.
[32] E. Hoyos, D. López, H. Alvarez, A phenomenologically based material fl ow model for friction stir welding, Mater. Des. 111 (2016) 321–330.
[33] U. Frevert, S. Engelmann, S. Zougbédé, J. Stange, B. Ng, K. Matuschewski, L. Liebes, H. Yee, Intravital observation of plasmodium berghei sporozoite infection of the liver, PLoS Biol. 3 (2005), e192.
[34] I. Magnusson, D.L. Rothman, B. Jucker, G.W. Cline, R.G. Shulman, G.I. Shulman, Liver glycogen turnover in fed and fasted humans, Am. J. Physiol. Endocrinol. Metabol. 266 (1994) E796–E803.
[35] T. Kenner, H. Hinghofer-Szalkay, H. Leopold, H. Pogglitsch, The relation between the density of blood and the arterial pressure in animal experiments and in patients during hemodialysis (author's transl), Zeitschrift fur Kardiologie 66 (1977) 399.
[36] N. Berndt, H.G. Holzhütter, Dynamic metabolic zonation of the hepatic glucose metabolism is accomplished by sinusoidal plasma gradients of nutrients and hormones, Front. Physiol. 9 (2018) 1786.
[37] H. Alvarez, Process Modeling for Analysis and Control. Dynamic Effects in Unitary Operations and Reactive Processes, In press, Universidad Nacional de Colombia, 2020.
[38] C. Fromentin, D. Tomé, F. Nau, L. Flet, C. Luengo, D. Azzout-Marniche, P. Sanders, G. Fromentin, C. Gaudichon, Dietary proteins contribute little to glucose production, even under optimal gluconeogenic conditions in healthy humans, Diabetes 62 (2013) 1435–1442.
[39] T. Ishida, J. Field, Hepatic handling of glucagon, in: Glucagon II, Springer, 1983, pp. 361–388.
[40] D. Raddatz, G. Ramadori, Carbohydrate metabolism and the liver: actual aspects from physiology and disease, Z. Gastroenterol. 45 (2007) 51–62.
[41] L. Lema-Perez, R. Muñoz-Tamayo, J. Garcia-Tirado, H. Alvarez, On parameter interpretability of phenomenological-based semiphysical models in biology, Inf. Med.Unlocked 15 (2019) 100158.
[42] R.H. Perry, D.W. Green, Perry's Chemical Engineers' Handbook, 8 ed., McGraw-Hill Professional, 2008.
[43] C. Guyton, A, J.E. Hall, Textbook of Medical Physiology, seventh ed., 2006.
[44] M. König, S. Bulik, H.G. Holzhütter, Quantifying the contribution of the liver to glucose homeostasis: a detailed kinetic model of human hepatic glucose metabolism, PLoS Comput. Biol. 8 (2012).
[45] R. Taylor, I. Magnusson, D.L. Rothman, G.W. Cline, A. Caumo, C. Cobelli, G. I. Shulman, Direct assessment of liver glycogen storage by 13C nuclear magnetic resonance spectroscopy and regulation of glucose homeostasis after a mixed meal in normal subjects, J. Clin. Invest. 97 (1996) 126–132.
[46] M.C. Moore, K.C. Coate, J.J. Winnick, Z. An, A.D. Cherrington, Regulation of hepatic glucose uptake and storage in vivo, Advances in nutrition 3 (2012) 286–294.
[47] K.N. Bojsen-Møller, A.M. Lundsgaard, S. Madsbad, B. Kiens, J.J. Holst, Hepatic insulin clearance in regulation of systemic insulin concentrations-role of carbohydrate and energy availability, Diabetes 67 (2018) 2129–2136.
[48] W.W. Lautt, Hepatic circulation: physiology and pathophysiology, in: Colloquium Series on Integrated Systems Physiology: from Molecule to Function, Morgan & Claypool Publishers, 2009, pp. 1–174.
[49] J.E. Gerich, Control of glycaemia, Bailliere. Clin. Endocrinol. Metabol. 7 (1993) 551–586.
[50] B.V. Kulkarni, R.D. Mattes, Lingual lipase activity in the orosensory detection of fat by humans, Am. J. Physiol. Regul. Integr. Comp. Physiol. 306 (2014) R879–R885.
[51] J. Boyle, D. Nelson, M. Cox, Lehninger Principles of Biochemistry, Wiley Online Library, 2005.
[52] M. Stumvoll, G. Perriello, C. Meyer, J. Gerich, Role of glutamine in human carbohydrate metabolism in kidney and other tissues, Kidney Int. 55 (1999) 778–792.
[53] A. Caumo, C. Cobelli, Hepatic glucose production during the labeled ivgtt: estimation by deconvolution with a new minimal model, Am. J. Physiol. Endocrinol. Metabol. 264 (1993) E829–E841.
[54] J.T. Sorensen, A Physiologic Model of Glucose Metabolism in Man and its Use to Design and Assess Improved Insulin Therapies for Diabetes (Ph.D. thesis), 1985.
[55] C. Dalla Man, R.A. Rizza, C. Cobelli, Meal simulation model of the glucose-insulin system, IEEE Trans. Biomed. Eng. 54 (2007) 1740–1749.
[56] R. Visentin, E. Campos-Náñez, M. Schiavon, D. Lv, M. Vettoretti, M. Breton, B. P. Kovatchev, C. Dalla Man, C. Cobelli, The uva/padova type 1 diabetes simulator goes from single meal to single day, J. Diabetes. Sci. Technol. 12 (2018) 273–281.
[57] E. Chalhoub, L. Xie, V. Balasubramanian, J. Kim, J. Belovich, A distributed model of carbohydrate transport and metabolism in the liver during rest and high-intensity exercise, Ann. Biomed. Eng. 35 (2007) 474–491.
[58] H.E. Silber, P.M. Jauslin, N. Frey, M.O. Karlsson, An integrated model for the glucose-insulin system, Basic Clin. Pharmacol. Toxicol. 106 (2010) 189–194.
[59] M. El-Refai, R.N. Bergman, Simulation study of control of hepatic glycogen synthesis by glucose and insulin, Am. J. Physiol.Legacy Content 231 (1976) 1608–1619.
[60] M. König, H.G. Holzhütter, Kinetic modeling of human hepatic glucose metabolism in type 2 diabetes mellitus predicts higher risk of hypoglycemic events in rigorous insulin therapy, J. Biol. Chem. 287 (2012) 36978–36989.
[61] R. Hovorka, V. Canonico, L.J. Chassin, U. Haueter, M. Massi-Benedetti, M. O. Federici, T.R. Pieber, H.C. Schaller, L. Schaupp, T. Vering, et al., Nonlinear model predictive control of glucose concentration in subjects with type 1 diabetes, Physiol. Meas. 25 (2004) 905.
[62] S. Panunzi, M. Pompa, A. Borri, V. Piemonte, A. De Gaetano, A revised sorensen model: simulating glycemic and insulinemic response to oral and intra-venous glucose load, PLoS One 15 (2020), e0237215.